JOURNAL OF MATERIALS SCIENCE 26 (1991) 5261–5268

Stress relaxation in wood: Scots pine veneer

Part II *Quantitative comparison with the prediction of a cooperative flow model*

D. G. KUBÁT
Department of Wood Technology, Royal Institute of Technology, S-100 44 Stockholm, Sweden

C. KLASON*
Department of Polymeric Materials, Chalmers University of Technology, S-412 96 Gothenburg, Sweden

Stress relaxation data obtained from samples of Scots pine veneer at different initial stress and humidity levels are presented. When plotted as stress (σ) against log time (t) the relaxation curves appear to be the result of a superposition of a largely linear portion and a tail which can be described by a single time exponential. The linear part of the σ against log t curve is reproduced using a modified version of a cooperative flow model. Agreement between theoretical and experimental data is excellent over the entire time range covered by the measurements. This includes the validity of the relation $F \approx 0.1\Delta\sigma$ between the slope of the linear part of the σ against ln t and the stress decrease produced by the corresponding mechanism. This relation is valid independent of the sample orientation, humidity and other variables; earlier, it has been shown to possess general validity for both polymers and metals. On the whole, relative humidity (up to about 95%) influenced the relaxation process relatively little, an exception to this being samples cut in the 45° direction where an appreciable increase in the relaxation strength with relative humidity was observed. The relaxation curves scaled in an approximately linear fashion with the initial stress.

1. Introduction

This paper is a continuation of a previous study of stress relaxation kinetics in wood (Scots pine veneer) [1]. The data presented therein, obtained at a relative humidity (r.h.) of about 50%, showed clearly that wood fits well into the general empirical pattern of stress relaxation kinetics observed in a large number of solids, and expressed by the relationship [2, 3]

$$F = (0.1 \pm 0.01)\Delta\sigma \quad (1)$$

Here F denotes the maximum (inflexion) slope of the stress (σ) against ln time (t) curves, and $\Delta\sigma$ is the total stress decrease during the relaxation process, a quantity also referred to as the initial effective stress σ_0^*, which equals the difference between the applied initial stress σ_0 and the equilibrium stress σ_∞ attained after sufficiently long measuring times. Equation 1 has been found to apply both to metals, polymers, and a number of other solids with widely different structures and compositions. Reaching a complete equilibrium in a stress relaxation process normally requires times significantly in excess of available measurement resources. This could be the reason why Equation 1 has not been given the attention it apparently deserves in view of its general validity.

In the preceding paper [1] the validity of Equation 1 was established for the longitudinal, transverse and 45° directions at about 50% r.h. using a simple graphical evaluation of the shape of the σ against log t curves. An important step was the separation of the two stages constituting the relaxation process in wood. As evident from the data presented earlier [1], and from the references given therein, a typical σ against log t curve appears to be the result of a superposition of the usual, largely linear σ against log t portion of the curves and of an additional stage where the stress decreases at a higher rate along the log t axis. While the first process has an equivalent extension of about four decades of time when approximated by a straight line, the second stage is significantly narrower, reminiscent of an $\exp(-kt)$ time-dependence (Maxwell relaxation). The empirical finding of a structure independent $F/\Delta\sigma$ ratio, Equation 1, relates to the first stage of the relaxation process which may also be called the main dispersion region. The significance of $\Delta\sigma$ for a compound process

* Author to whom correspondence should be addressed.

0022–2461/91 $03.00 + .12

found in experiments with wood will be explained below.

In the present paper the shape of the relaxation curves is analysed using a modified version of a co-operative flow model for the main (first) region superimposed on an $\exp(-kt)$ process to fit the tail of the curves. When the theoretical slope F is adjusted to Equation 1, good agreement between theory and experimental data is obtained. On the other hand, the parameters of the exponential tail had to be found empirically. The applicability of Equation 1 was verified for samples cut in the longitudinal (L), transversal (T), and 45° direction within a humidity range covering approximately 20–95% r.h. (somewhat different ranges for different directions). A fair degree of agreement with experimental data was achieved when fitting the tail of the relaxation curves using a single time exponential.

References to literature dealing with the stress relaxation process in wood were cited in [1]. We concluded there that the main part of the published work did not fulfill the requirements of physically well defined measurements, especially with regard to the constancy of the humidity of the surrounding atmosphere. Qualitatively, however, when plotted as σ against $\log t$ the relaxation curves, in most cases, exhibited features similar to those found in the present work, and also in [1]. This relates, in the first place, to the general shape of such curves, showing a main dispersion region extending over about four decades of time, followed by a more rapid decline corresponding approximately to a simple Maxwellian process [4]. Similar results have been reported in [5] but not cited in [1]. This is also the case with [6], dealing mainly with creep, but supplemented with some data on relaxation for samples of Tasmanian mountain ash. The authors observed that the extent of relaxation increased with relative humidity. The curves were plotted on a linear time scale which obscured the true character of the kinetics of the process. A theoretical analysis of the results in terms of the theory of stress-dependent thermal activation is dealt with in a subsequent paper [7]. Stress against time plots were also used in [8], relating to the behaviour of red oak in tension and compression. In general, the extent of relaxational flow appeared to be smaller in the latter loading mode. Relaxation curves measured on coniferous tissues (microspecimens), presented in [9], show that the course of the stress decay depends strongly on sample location and the loading mode (tension against compression). Some experimental contributions to the relaxation process in cork have been published recently [10]. However, the results obtained do not allow a quantitative evaluation.

2. Experimental procedure

The experiments were carried out largely in the same way as described previously [1]. The samples were obtained from a radially cut splint veneer of Scots pine (*Pinus silvestris*). The effective length of the rectangular samples was 6 cm; their width 3, 6, or 12 mm, and thickness 0.75–0.80 mm. The distance between the growth rings was 1.4 ± 0.1 mm, the proportion of latewood $24 \pm 3\%$, the density 0.49 g cm^{-3} at 50% r.h., and the humidity content 8.1% at the same r.h. level.

Similar to the findings of [1], the modulus values calculated from the initial slope of the stress–strain curves preceding the relaxation showed a comparatively large scatter. With relatively small samples this was to be expected. At the 50% r.h. level the modulus values were identical to those reported in [1], that is to say 9.4 ± 1.4, 0.57 ± 0.15, and 0.20 ± 0.05 GPa in the L, 45°, and T-directions. Increasing the r.h. to 95% reduced the L-modulus to approximately 7 GPa. In the other two directions the variation of r.h. within the ranges evident from, for instance, Fig. 6, did not produce any statistically significant modulus variation. The scatter in these data was rather high.

The measuring equipment, consisting of two identical relaxometers, has been described in [1]. The relaxometers had a considerably higher stiffness than normal tensile testing equipment usually employed for measurements of this type. The strain rates used were 8.3×10^{-3} and 7.1×10^{-4} s^{-1}; they did not affect the results in any measurable way. The straining times corresponding to the initial deformation of the samples are given in Table I which specifies the data for the relaxation curves reproduced in Figs 2–4. The results were not influenced by the width of the samples.

Varying levels of r.h. were produced by circulating air through a number of flasks containing glycerol/water mixtures of the appropriate concentration in a closed circuit through the cabinet in which the relaxometers were contained.

The constancy of the humidity level in the cabinet during the period of measurement was constantly checked using an Assmann psychrometer and an electronic hygrometer (Rotronic, type I 128). Other details of the measuring procedure can be found in [1].

3. Theoretical background

When modelling the stress relaxation process in wood, one has to take account of the fact that the shape of the relaxation curves, when plotted as σ against $\log t$, appears to be the result of a superposition of two mechanisms, a sigmoid curve generally, and a tail reminiscent of an exponential stress decay, that is to say $\sigma \propto \exp(-kt)$, or $\log \sigma \propto t$. Fig. 1 shows in a schematic fashion a superposition of the two mechanisms, their contributions to the total stress decrease being denoted σ_{10} and σ_{20}, respectively. After a sufficiently long time an equilibrium state, characterized by the stress level σ_∞, is reached. Apparently

$$\sigma_{10} + \sigma_{20} + \sigma_\infty = \sigma_0 \qquad (2)$$

with σ_0 denoting the initial stress applied to the sample.

The various theoretical approaches used in describing the relaxations process in solids, discussed in [1], included the theory of stress-dependent thermal activation (SDTA). This reproduces the observed linearity of the curves well when plotted in σ against $\log t$

TABLE I Experimental conditions and parameters entering Equation 8 for a typical selection of stress relaxation experiments. The corresponding curves are reproduced in Figs 2–4. (σ_0) initial stress, (σ_{10}) contribution of the linear σ against $\log t$ mechanism, (σ_{20}) contribution of the exponential tail, (σ_∞) equilibrium stress, (τ, α) time constants limiting the extension of the linear σ ($\log t$) part, (τ_2) time constant of the exponential tail, (t_1) straining time, (ε_0) initial deformation. The ratio τ/α chosen in accordance with Equation 1, i.e. $\ln \tau/\alpha = 10$. The values of σ_{10}, σ_{20}, σ_∞, τ, and τ_2 obtained by fitting Equation 8 to experimental data

No.	Orientation	r.h.	σ_0 (MPa)	σ_{10}/σ_0 (%)	σ_{20}/σ_0 (%)	σ_∞/σ_0 (%)	τ (10^3 s)	α	τ_2 (10^3 s)	t_1 (s)	ε_0 (%)
1	L	0	0.90	5.4	32.1	62.5	3.85	0.17	165	1.02	0.043
2	L	84.7	2.27	11.9	8.9	79.2	1.35	0.061	50	0.54	0.038
3	L	93.5	2.46	10.8	12.5	76.6	18	0.82	175	0.76	0.032
4	L	94.5	6.03	18.0	21.5	60.5	14	0.64	35	1.06	0.073
5	L	94.2	12.3	19.7	14.2	66.1	54	2.45	100	1.85	0.128
6	L	74.7	15.3	9.8	7.1	83.2	10	0.45	72	2.47	0.171
7	L	65.3	16.8	10.0	5.9	84.1	80	3.63	600	5.25	0.35
8	L	58.9	35.6	11.7	6.7	81.6	45	2.04	700	4.1	0.28
9	L	40.0	66.7	14.1	28.8	57.1	5	0.23	420	5.64	0.78
10	T	63.9	1.44	26.7	12.7	60.6	27.5	1.25	100	10.3	0.71
11	T	71.8	1.66	17.1	8.6	74.3	4.5	0.20	53.5	1.15	0.86
12	T	92.4	1.85	50.6	16.5	32.9	5.0	0.23	10	1.8	1.5
13	T	24.5	1.89	22.7	20.5	56.8	6.2	0.28	58	0.99	0.83
14	T	37.8	2.10	23.5	14.1	62.3	5.0	0.23	42	0.96	0.80
15	T	17.0	2.10	21.4	18.6	60.0	6.4	0.29	44	0.96	0.80
16	T	33.2	2.97	28.6	17.2	54.2	7.5	0.34	55	1.82	1.52
17	T	72.0	3.38	24.6	10.1	65.3	4.25	0.19	45	1.30	1.08
18	45°	59.4	0.94	15.9	0.4	83.7	35	1.59	10	2.4	0.15
19	45°	55.4	1.50	16.5	7.1	76.4	3.75	0.17	45	0.58	0.43
20	45°	94.0	2.09	57.7	16.6	25.7	57.5	2.61	75	13.0	0.54
21	45°	94.7	2.09	58.3	19.4	22.3	64	2.91	150	9.7	0.40
22	45°	93.5	2.27	59.1	17.4	23.5	50	2.27	105	14.2	0.59
23	45°	74.3	3.12	21.4	14.4	64.2	7.0	0.32	210	0.53	0.44
24	45°	78.4	3.30	32.7	16.4	50.9	17.5	0.79	150	0.52	0.43

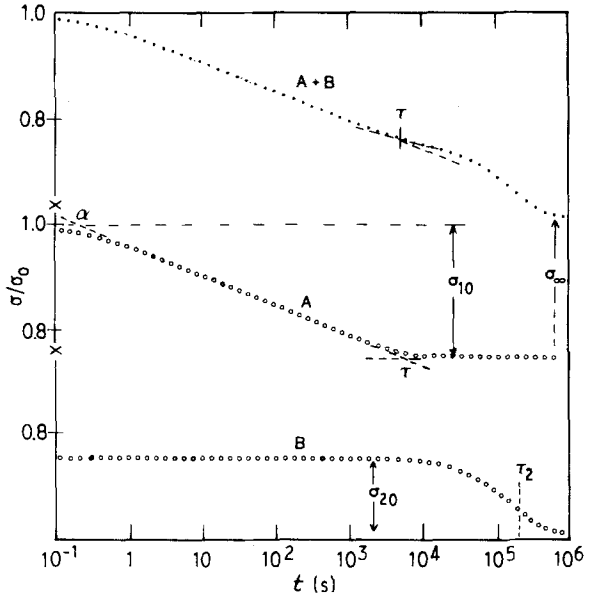

Figure 1 Schematic representation of the two mechanisms A and B producing the compound curve (A + B in the figure) used to fit experimental data. The cooperative mechanism A corresponds to a largely linear σ against $\log t$ curve, mechanism B is the exponential tail, *cf.* Equation 8. The curves A and B are shifted arbitrarily downwards in order to avoid overlap. The σ/σ_0 scale is shown to the right. The parameters used in this superposition are as follows: $\sigma_{10}/\sigma_0 = 24.5\%$, $\sigma_{20}/\sigma_0 = 14.0\%$, $\sigma_\infty/\sigma_0 = 61.4\%$, $\tau = 5000$ s, $\alpha = 0.227$ s, $\tau_2 = 180000$ s, $F/\sigma_{10} = 0.1$ (applies to mechanism A).

diagrams [11]. This is a consequence of the exponential dependence of the stress rate $d\sigma/dt$ on the stress. However, since this theory does not distinguish between the stress dependence of $d\sigma/dt$ during a relaxation process and the dependence when the stress initially applied to the sample is changed, it cannot reproduce the linear scaling of the relaxation curves with regard to the initial stress, which was one of the main findings of our earlier work and also a general feature of the relaxation process in solids. The second main approach to describing phenomena of this kind uses a spectrum of relaxation times. This is a purely formal method not giving any information in addition to that following directly from the shape of the σ against $\log t$ plot, since the spectrum is obtained by differentiating such plots with respect to $\log t$ [12].

An approach which has recently shown considerable promise in understanding relaxation processes in common solids is based on a cooperative model with a particularly simple interaction mechanism reminiscent of that encountered in Bose-Einstein statistics [13, 14]. An important advantage of this model is its ability to describe the linear scaling of the process with respect to the initial stress σ_0, at the same time as it yields an exponential relation between $\dot{\sigma}$ and $\sigma(t)$ as required by the linearity of the σ against $\log t$ plots.

The theoretical model to be described here is based on a superposition of the following two processes:

Mechanism I: $\sigma \propto \log t$, and
Mechanism II: $\sigma \propto \exp(-kt)$,

contributing to the total stress decrease with σ_{10} and σ_{20}, respectively.

The first stage of the relaxation process is modelled using a modified version of the cooperative model

[13, 14] based on the assumption that the elementary events constituting the macroscopic process occur in clusters of varying size. The underlying mechanism is assumed to be the transition of the flow units from the stressed to the relaxed state. The phonons liberated during such transitions may then induce transitions of yet unrelaxed flow units, thus producing multiple (clustered) transitions in keeping with their bosonic character. This leads to a particular form of the distribution of relaxation times, reproducing well the observed behaviour. In general, the physical nature of the flow units is not known. They may be entities such as dislocations in metals, chain segments in polymers etc.

Here we replace the clustering mechanism with a nonlinear differential equation reminiscent of the Malthus-Verhulst scenario, and applied to the time derivative of the quantity (stress, number of flow units) under discussion.

Let us assume that the movement of the flow units is hindered by interactions with their surroundings. Restrictions on the mobility of structural elements in solids are well known, and the key role of the free volume in theories of solid state flow, physical ageing etc. is well established [15]. The following differential equation appears to describe such a situation in a natural way,

$$\frac{d\dot{n}}{dt} = a\dot{n} + b\dot{n}^2 \tag{3}$$

or,

$$\frac{d\dot{n}}{dt} = a\dot{n}(1 + b\dot{n}/a) \tag{4}$$

where $\dot{n} = dn/dt$, the rate of change in the number of unrelaxed units n, a quantity assumed to be proportional to the unrelaxed stress. After integration we obtain for $\dot{n}$

$$\dot{n} = \dot{n}_0/[(1 + b\dot{n}_0/a)\exp(-at) - b\dot{n}_0/a] \tag{5}$$

and for $n(t)$ the final expression

$$n = n_0 - \frac{1}{b}\ln[1 + (b\dot{n}_0/a) - (b\dot{n}_0/a)\exp bt] \tag{6}$$

where n_0 is the number of unrelaxed units at $t = 0$. The constant a (negative) has the usual meaning of a rate constant of first order chemical kinetics, and b (positive) is a measure of the mutual induction effect (cooperation). Equations 3 to 6 relate to a situation where the cooperative effect is due to flow units undergoing transitions to the unstressed state and not, as in the SDTA theory, by the ensemble of all unrelaxed units.

An important parameter characterizing the shape of the σ against $\log t$ curve is the slope

$$F = \left[\frac{d\sigma}{d(\ln t)}\right]_{max} \tag{7}$$

appearing in Equation 1.

In the computer evaluation of the experimental material we did not determine directly the inflexion slope of the main dispersion region as was the case in [1]. Instead, in order to characterize the extension of the relevant portion of the curves, we used the ratio of the corresponding time intercepts, since this ratio appears in a natural way in the final formula used to fit the experimental data, *cf.* Equation 8 below and Fig. 1. The basis of this procedure is as follows.

When approximating the curve by a straight σ against $\log t$ line one obtains two time constants, α and τ, intercepting the time axis at $\sigma = \sigma_0$ and $\sigma = \sigma_0 - \sigma_{10}$, respectively, as indicated schematically in Fig. 1. Here $\sigma_0 - \sigma_{10}$ is the equilibrium stress of the main relaxation region as described by Equations 3 to 6. Since $F = \dot{\sigma}t$ along the linear σ against $\log t$ extrapolation, *cf.* Equation 7, we obtain $F \approx \dot{\sigma}_0\alpha$ for the value of the intercept α of the straight line approximation with $\sigma = \sigma_0$. The second intercept τ of this line with $\sigma = \sigma_0 - \sigma_{10}$ can be shown to be approximately equal to the inverse value of the rate constant $|a|$ appearing in Equations 3 to 6. The error incurred in equating τ and $|1/a|$ is negligible for σ against $\log t$ curves obeying Equation 6 and extending over about four decades of time, as required by Equation 1. Omitting the calculational details, we now recast Equation 6 in the following form, at the same time including an exponential term describing the rapidly declining stress in the tail portion of the $\log t$ curves

$$\frac{\sigma(t)}{\sigma_0} = \frac{\sigma_{10}}{\sigma_0} - \frac{\sigma_{10}}{\sigma_0 \ln(\tau/\alpha)} \times \ln\left[1 + \frac{\tau}{\alpha} - \frac{\tau}{\alpha}\exp\left(-\frac{t}{\tau}\right)\right] + \frac{\sigma_{20}}{\sigma_0}\exp\left(-\frac{t}{\tau_2}\right) + \frac{\sigma_\infty}{\sigma_0} \tag{8}$$

Here the numbers of the relaxing units have been replaced by the corresponding stresses, and the equation normalized with respect to σ_0. The second term on the right hand side describes the largely linear portion of σ against $\log t$, the third term the exponential tail. We further note that in Equation 8 the ratio $b\dot{n}/a$ of Equation 6 has been replaced by τ/α, defining the extension of the main σ against $\log t$ region when approximated by a straight line.

When fitting Equation 8 to experimental data the ratio τ/α has been taken to fit Equation 1 requiring that $F = 0.1(\sigma_0 - \sigma_{20} - \sigma_\infty) = 0.1\sigma_{10}$. This corresponds to $\ln\tau/\alpha = 10$ or $\tau/\alpha = \exp(10)$. With regard to the first mechanism, all the theoretical curves reproduced in Figs 2–4 strictly comply with Equation 1. Appropriate values of τ had to be chosen. This does not detract from the general validity of Equation 1 since τ only affects the position of the curves along the $\log t$ axis. With regard to the second mechanism, both τ_2 and σ_{20} had to be selected so as to fit the experimental data. The fitting procedure was carried out using a computer.

4. Results

In this section we present a number of examples of the relaxation kinetics as observed with the pine veneer samples used. The results, reproduced as σ/σ_0 against $\log t$ diagrams, are compared with theoretical relaxation curves calculated from Equation 8. As already

mentioned, the theoretical approach consists of superimposing a largely linear σ against $\log t$ mechanism and an exponential tail. The experimental data relate to varying conditions of initial stress and relative humidity applied to samples cut in L, T, and 45° directions.

The experimental plots for σ against $\log t$ in Figs 2–4 are approximately linear over a significant portion of the logarithmic time. Their final portion is characterized by a steeper stress decline. In this respect the results shown in Figs 2–4 are similar to those reported in [1] relating to an r.h. value of about 50%. The two mechanisms appearing in Equation 8 are assumed to act independently of each other. In some cases, it was not necessary to take account of the second mechanism in order to obtain a fair agreement with the experimental results.

The curves reproduced in Figs 2–4 show a high degree of agreement with the corresponding theoretical data. When fitting Equation 8 to the experimental material the slope F was chosen to comply with Equation 1, that is

$$F/\sigma_{10} = 0.1 \qquad (9)$$

for all the theoretical plots reproduced in Figs 2–4. This amounts to specifying the ratio of the two limiting time constants α and τ to be $\tau/\alpha = \exp(10)$, *cf.* Fig. 1. The only arbitrary steps in the fitting procedure were a proper selection of τ (or α) and of σ_{10}. The first of these quantities specifies the position of the $\sigma(\log t)$ curve along the log time axis and the second the total stress decrease associated with the main process. There appears to be no possibility of predicting these values on physical grounds. The exponential tail of the curves had to be fitted empirically both with regard to its position (τ_2) and the corresponding stress decrease (σ_{20}).

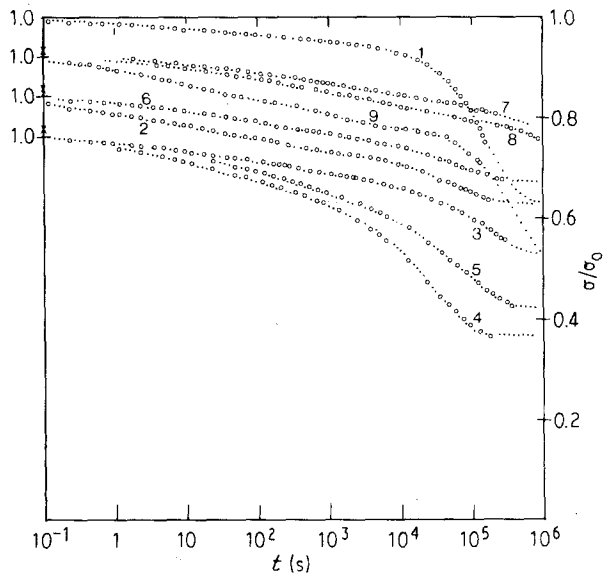

Figure 2 Experimental (open symbols) and theoretical (dots) relaxation curves for samples cut in the longitudinal direction. Theoretical curves based on Equation 8 with the condition $F/\sigma_{10} = 0.1$, Equation 1. Other parameters chosen to produce best fits. Some of the curves have been shifted vertically for clarity. The numbers relate to experimental conditions given in Table I.

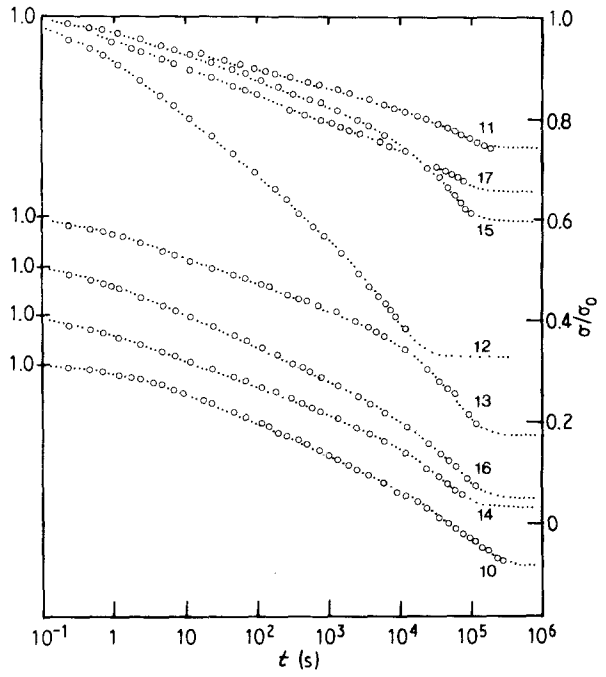

Figure 3 As for Fig. 2 but with samples cut in the transverse direction.

Considering the fact that a prescribed value of F/σ_{10}, that is 0.1, has been used in all the theoretical curves, the agreement with the measured values is truly amazing. This applies to all three orientations of the samples, and also to the varying conditions of initial stress and relative humidity. Although minor deviations are found in some cases, they are well accommodated within the scatter of $\pm$ 10%. In certain cases the superposition of the two relaxation processes may in certain cases distort the σ against $\log t$ linearity of the first mechanism as found, for instance, with some samples cut in the 45° direction. However, this does not appear to influence the overall agreement between calculated and experimental data.

As discussed in detail in [1] the curves for σ against $\log t$ scale approximately linearly with the initial applied stress σ_0. This applies both to the slope F and to

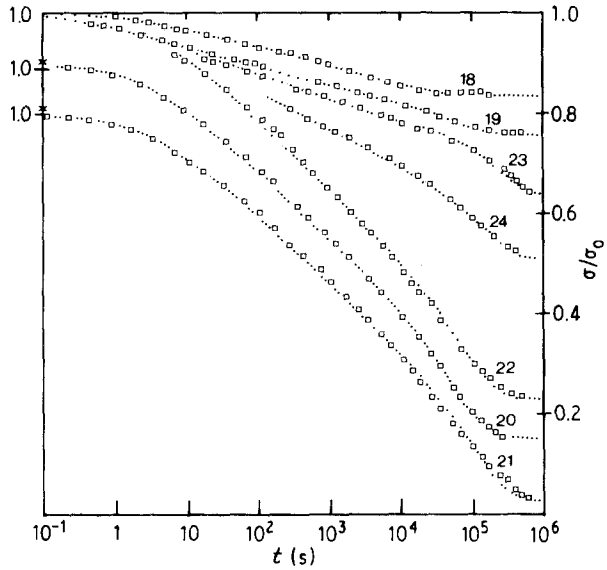

Figure 4 As for Fig. 2 but with samples cut in the 45° direction.

the stress decrease σ_{10} relating to the first relaxation mechanism, since these quantities are related through Equation 1. We demonstrate this linearity by plotting σ_{10} against the total initial stress σ_0, in Fig. 5. Since F was chosen as 0.1 of σ_{10}, plotting F instead of σ_{10} against σ_0 would only amount to a change of scale.

Apart from σ_{10} against σ_0, Fig. 5 also contains plots of σ_{20}, the stress decrease relating to the second (exponential) mechanism, and σ_∞, the calculated equilibrium stress, against the initial stress σ_0. All these quantities appear to scale linearly with σ_0, irrespective of the orientation of the samples (L, T, and 45°). In some instances an appreciable scatter is noted, an effect likely to be related to the heterogeneity of the samples in relation to their size, and to varying r.h. This explains why the scatter of the data in Fig. 5 is higher than that found in [1] where the humidity was constant. The occurrence of data relating to various humidity levels is a factor complicating a direct assessment of the results shown in Fig. 5. Apart from this, the linear scaling of σ_{10}, σ_{20}, and σ_∞ with regard to the total initial stress σ_0 is still evident. Some of the points in the diagrams of Fig. 5 relating to the highest humidity levels have been marked correspondingly in order to illustrate the role of r.h. As could be expected the slope of the diagrams showing $\sigma_{10}(\sigma_0)$ and $\sigma_{20}(\sigma_0)$ increased with the humidity.

As a supplement to Fig. 5 we show the dependence of σ_{10}, σ_{20}, and σ_∞ on r.h. in Fig. 6. The experimental points relate to various levels of σ_0. Since we attempt only to illustrate the role of humidity in influencing the various contributions to the relaxation process, we do not specify the σ_0 values. The σ_{10}, σ_{20}, and σ_∞ data have been normalized with regard to σ_0.

Disregarding the role of σ_0, which is not evident from the diagrams of Fig. 6, we find that the σ_{10}/σ_0 values in the L and T directions are affected relatively little by the humidity. In the 45° direction, however, a significant increase in σ_{10}/σ_0 with the humidity is found. The fact that we have not specified σ_0 in Fig. 6 does not affect such a conclusion. This is confirmed by inspecting the shape of the σ against $\log t$ curves for the 45° samples in Fig. 4. We find there that the total stress decrease observed with such samples at high humidities is significantly above the levels measured in the other two directions, indicating a shear-related flow mechanism.

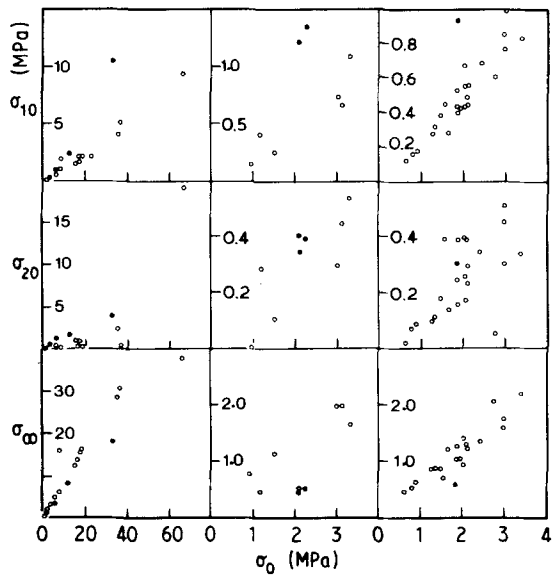

Figure 5 The variation of the stress components σ_{10}, σ_{20}, and σ_∞ with the initial stress for samples tested at different humidities. Left—longitudinal; middle—45°; and right—transverse direction. Filled points—r.h. in excess of 95%.

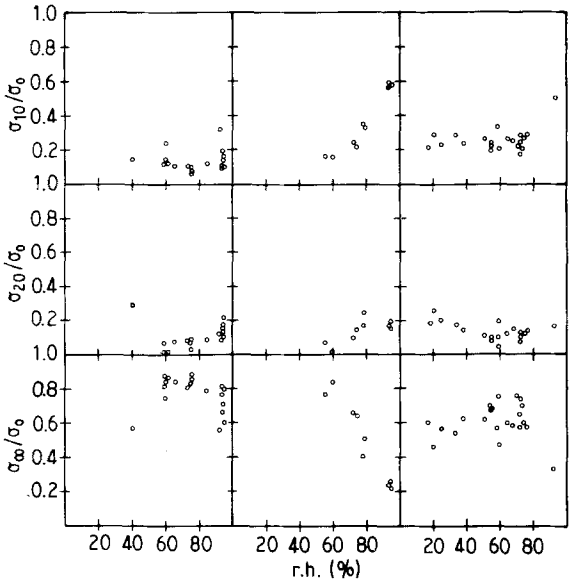

Figure 6 Influence of relative humidity on the stress components σ_{10}, σ_{20}, and σ_∞ normalized with regard to σ_0. Varying σ_0 level. Left—longitudinal; middle—45°; and right—transverse direction.

With regard to the humidity dependence of the normalized ratio σ_{20}/σ_0, Fig. 6, the pattern of the experimental points does not show any particular features, the value of σ_{20}/σ_0 changing comparatively little.

The calculated equilibrium stress σ_∞ varies with the humidity in a simple manner only for the 45° samples. This is to be expected, since σ_∞ in itself is not an independent quantity, Equation 2. We note that at the highest r.h. levels the equilibrium stress can be as low as about 20% of σ_0. In this respect the 45° samples stand out as rather special. In order to facilitate a quantitative assessment of the experimental material we present in Table I the values of the parameters entering Equation 8 along with the experimental conditions used when recording the curves reproduced in Figs 2–4. Although the data in this table represent only a minor part of the experiments carried out in this study, we consider them to be sufficient in this context. To represent all the data relating, for instance, to Figs 5 and 6, would by far exceed available space.

5. Discussion

The validity of Equation 1, as demonstrated by the data shown in Figs 2–4, stands out as an interesting finding, especially since we have here a case of a material exhibiting a superposition of two different relaxation mechanisms. Using Equation 8 to fit the experimental results eliminated possible ambiguity in the graphical evaluation used to demonstrate the

validity of Equation 1 in our preceding paper [1]. As explained above, only the values of τ, that is to say the expected lower intercept of σ against $\log t$ with $\sigma_o - \sigma_{10}$, and of σ_{10} had to be selected. Once this position is fixed, the slope of the σ against $\log t$ curves is determined by Equation 1. Equation 1 remains valid when the humidity of the surrounding atmosphere is changed within relatively wide limits in all three sample directions investigated.

The occurrence of the second mechanism, confined to a relatively narrow range of the $\log t$ axis, appears to be a characteristic feature of the relaxation process in wood [1, 4, 5]. Here, we have achieved a fair degree of agreement with experimental data when considering it as a simple time exponential superimposed on the mechanism defined by Equation 1. It is conceivable that other expressions such as a stretched exponential or a power law, would have given even better results. However, for the present purpose the fit is more than satisfactory, even though the rapid approach to equilibrium of a simple exponential may appear somewhat idealized.

As a supplement to the computer-aided application of Equation 8 to the experimental material we also used the simple graphical procedure as described earlier [1]. In this way the value of F/σ_{10} was found to be 0.10 ± 0.012. Similar results were obtained when using the graphically determined values of F and the σ_{10} values emerging from the computerised fitting procedure. These results should provide additional support for the conclusions pertaining to Equation 1. One should also appreciate the fact that the evaluation of the results encompassed a separation of the relaxation process into two components, a procedure which one would expect to affect the final results in an adverse manner.

Another feature of the data is the linearity with regard to the total applied stress σ_o. Apart from the scatter appearing in certain of the diagrams shown, such linear scaling is evident for all the three parts of which σ_o is composed, Equation 2. This rules out a direct application of theories of the SDTA type since they assume an exponential $\dot{\sigma}(\sigma)$ relation in which a linearity with respect to σ_o cannot be accommodated. This has been discussed in detail in [1], together with the main implications of the linear scaling concept.

Normally, stress relaxation in polymers and metals does not produce the narrow tail region found in wood. The initial stress σ_o thus only has two components (σ_{10} and σ_∞). When the main dispersion region (σ_{10}) scales linearly with σ_o, also σ_∞ does so. When we deal with three components it is not trivial to find that all of them are linear functions of σ_o. However, as our data show, this appears to be the case. An example of the linearity under discussion is Fig. 7, where σ_{20} has been plotted against σ_{10}, again without considering the role of relative humidity and the scatter caused thereby (samples cut in transverse direction). The correlation between corresponding data in the L and 45° directions was significantly weaker.

Although the approach to equilibrium is incomplete in most of the σ against $\log t$ curves shown in Figs 2–4, it can be seen that a simple time exponential

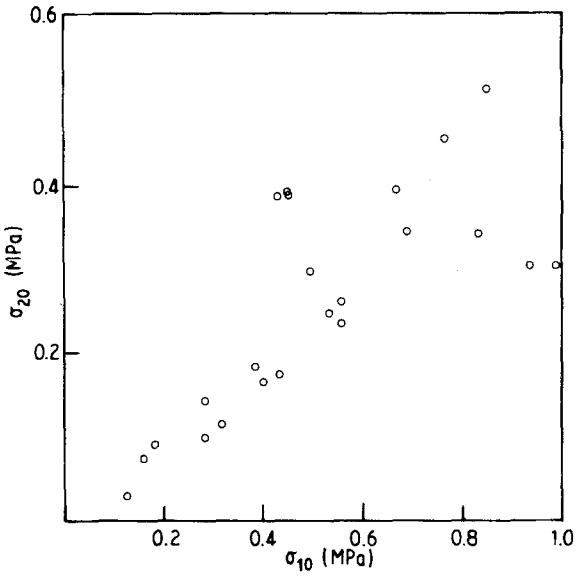

Figure 7 The relationship between σ_{20} and σ_{10} as found with the transversally cut samples. Points to the far right relate to experiments at r.h. levels exceeding 90%.

reproduces the second relaxation mechanism comparatively well. When constructing the equivalent of Equation 1 for this second stage we arrive at the trivial relation

$$\left[\frac{d\sigma}{d \ln t}\right]_{max} = \frac{\sigma_{20}}{e} \tag{10}$$

valid for any Maxwellian relaxation. Although the physical reason for the exponential tail is not known, it is plausible to associate it with diffusion of the moisture present in the samples. Experiments with completely dry samples have yet to be carried out.

When analysing the position of the two dispersion mechanisms along the time axis, as determined by the two time constants τ and τ_2, the data obtained showed appreciable scatter. This was true of the dependence of these constants on both σ_o and r.h. In general, the correlations were rather weak, not allowing any definite conclusions to be drawn. This implies, in turn, that σ_o and r.h. did not have any pronounced effect on the two time parameters. Since these matters are not of any particular importance in the present context, the corresponding diagrams are not shown here.

When discussing the validity of Equation 1, it may be appropriate to mention the so called stretched exponential, or the KWW formula (Kohlrausch-Williams-Watts) often used to describe relaxation, ageing and other processes extending over several decades of time. Such an exponential is a modification of the Maxwell formula [15]

$$\sigma = \sigma_o \exp(-kt^\beta) \tag{11}$$

where the exponent $\beta < 1$ is a measure of the extension along $\log t$. The normalized slope F of such a process is

$$\frac{F}{\sigma_o} = \frac{\beta}{e} \tag{12}$$

giving for β a value of 0.27 when Equation 1 is obeyed. In fact, values in the vicinity of 1/3 have been observed for polymers at temperatures sufficiently below the glass transition region [15]. This provides independent support to the notion that the flow mechanism underlying Equation 1, although yet unknown, is of a rather general physical significance. It certainly does not encourage attempts to interpret solid state flow in terms of independent events determined by molecular parameters such as in the SDTA concept [11]. Were that a plausible mechanism, it would be difficult to explain the similarities characterizing the relaxation process in such dissimilar groups of materials as wood, polymers and metals.

In conclusion, the exponential tail characteristic of the relaxation curves measured on wood samples is a highly unusual phenomenon not encountered with other materials including, for instance, wool fibres of varying humidity content [16]. It is not without interest in the present context to mention that Equation 1 has recently been shown to apply also in that case.

Acknowledgement

Financial support from the Swedish National Board for Technical Development is gratefully acknowledged.

References

1. D. G. KUBÁT, S. SAMUELSSON and C. KLASON, *J. Mater. Sci.* **24** (1989) 3541.
2. J. KUBÁT, *Nature* **204** (1965) 378.
3. J. KUBÁT and M. RIGDAHL, in "Failure of Plastics", edited by W. Brostow and R. D. Corneliussen (Hanser Publishers, New York, 1986) p. 60.
4. P. GROSSMAN, *Nature* **173** (1954) 42.
5. H. URAKAMI and K. NAKATO, Proceedings of the 14th Meeting of the Jap. Wood Res. Soc. Tokyo, April, 1964.
6. R. S. T. KINGSTON and L. N. CLARKE, *Austr. J. Appl. Sci.* **12** (1961) 211.
7. *Idem, ibid.* **12** (1961) 228.
8. R. L. YOUNGS, Forest Prod. Lab. Madison, WI, Report 2079 (1957).
9. E. KIRBACH, L. BACH, R. W. WELLWOOD and J. W. WILSON, *Wood and Fiber* **8** (1976) 74.
10. M. E. ROSA and M. A. FORTES, *J. Mater. Sci.* **23** (1988) 35.
11. A. S. KRAUSZ and H. EYRING, "Deformation Kinetics" (Wiley Interscience, New York, 1975).
12. A. V. TOBOLSKY, "Properties and Structure of Polymers" (Wiley, New York, 1960).
13. Ch. HÖGFORS, J. KUBÁT and M. RIGDAHL, *Phys. Status Solidi, B* **107** (1981) 147.
14. J. KUBÁT, *ibid.* **111** (1982) 599.
15. L. C. E. STRUIK, in "Failure of Plastics", edited by W. Brostow and R. D. Corneliussen (Hanser Publishers, New York, 1986) p. 209.
16. F.-J. WORTMAN, *Colloid & Polymer Sci.* **265** (1987) 126.

Received 30 May 1990
and accepted 31 January 1991